We review some aspects of the bipolar molecular outflow phenomenon. In particular, we compare the morphological properties, energetics, and velocity structures of outflows from high- and low-mass protostars and investigate to what extent a common source model can explain outflows from sources of very different luminosities. Many flow properties, in particular the CO spatial and velocity structure, are broadly similar across the entire luminosity range, although the evidence for jet entrainment is still less clear-cut in massive flows than in low-mass systems. We use the correlation of flow momentum deposition rate with source luminosity to estimate the ratio f of mass ejection to mass accretion rate. From this analysis it appears that a common driving mechanism could operate across the entire luminosity range. However, we stress that for the high-mass YSOs, the detailed physics of this mechanism and how the ejected wind/jet entrains ambient material remain to be addressed. We also briefly consider the alternative possibility that high-mass outflows can be explained by the recently proposed circulation models, and we discuss several shortcomings of those models. Finally, we survey the current evidence on the nature of the shocks driven by YSOs during their pre-main-sequence evolution.

I. INTRODUCTION

Stars of all masses undergo energetic, generally bipolar, mass loss during their formation. Diagnostics of mass loss using optical and near-infrared line emission provide the most dramatic images of the violent birth of stars,

but molecular flows, predominantly traced by their CO emission lines, provide the strongest constraints on models of cloud collapse and star formation, because molecular flows are the massive and predominantly cool reservoir where most of the flow momentum is eventually deposited and so provide a fossil record of the mass loss history of the protostar. In contrast, the optical and near-infrared emission arises from hot shocked gas, which cools in a few years and hence traces only the currently active shocks in the flow. In addition, because there is negligible extinction at millimeter wavelengths, even the youngest, most deeply embedded objects can be studied.

Since the last review of this subject in the *Protostars and Planets III* conference proceedings (Fukui et al. 1993), many breakthroughs in understanding the nature of these objects have been forthcoming, primarily as a result of improvements at millimeter- and submillimeter-wavelength observatories; we refer the reader in particular to volume 1 of the *Revista Mexicana de Astronomía y Astrofísica Conference Series* (Pismis and Torres-Peimbert 1995) and the proceedings of IAU Symposium 182 (Reipurth and Bertout 1997). More sensitive receivers and focal-plane arrays have allowed wide-field imaging of outflows, showing that they often extend to many parsecs in size, sometimes even beyond their natal cloud boundaries (e.g., Padman et al. 1997). In addition, the availability of mosaicked interferometric images of many outflows at 1–2″ resolution has led to significant breakthroughs in understanding the small-scale structure of outflows (e.g., Bachiller et al. 1995; Cernicharo and Reipurth 1996; Gueth et al. 1996) and provide strong constraints on viable outflow-acceleration models, in particular on the role of jets and the nature of the entrainment mechanism (Cabrit et al. 1997; Shu and Shang 1997). Finally, multiline studies (Bachiller and Pérez Gutiérrez 1997) have shown that shocks driven by flows chemically process the interstellar medium (ISM) at a rapid rate, modifying its composition and having profound implications for chemical and dynamical models of molecular clouds.

In this chapter we review some of the recent results on outflows from both low- and high-mass protostars and focus on a comparison of their physical properties. In section II we summarize the observed flow morphologies and velocity structures and look for evidence that a common mechanism could reproduce the observations of all such flows. In section III the possible entrainment and ejection mechanisms for outflows are addressed, and the evidence for a common mechanism is discussed based on an analysis of the flow energetics. Finally, in section IV the evidence for, and nature of, shocks in outflows is presented.

II. OUTFLOW STRUCTURE

Molecular outflows come in a wide variety of shapes and sizes. This is hardly surprising, given the likely diversity in the mass and multiplicities of the driving protostars, the outflow ages, and molecular environments.

Although at least 200 outflows have been cataloged (Wu et al. 1996), there is still no large homogeneous sample that has been mapped with good resolution and sensitivity, so much of our current understanding is heavily influenced by a few well-studied examples. This is even more true for high-mass systems, where perhaps only 10 or so outflows have been studied in detail, although rapid progress is being made using millimeter-wave interferometers to study flows in the often complex environment of high-mass star formation (Shepherd et al. 1998). Consequently, our current estimates of "typical" outflow properties may be far from accurate.

A. Low-mass Systems

It is now clear that stellar jets, with speeds of 100–300 km s^{-1} and densities of order 10^3 cm^{-3}, are responsible for accelerating much of the molecular gas in many of the youngest low-mass outflow systems (e.g., Richer et al. 1992; Padman and Richer 1994; Bachiller et al. 1995). However, there is also good evidence for momentum being deposited into the flows by wind components with wider opening angles and that this component perhaps becomes relatively more powerful as the flows age (e.g., Bence et al. 1998).

Some of the first clear evidence for a jet-dominated outflow origin was identified in the flows from L1448C (Bachiller et al. 1990; Guilloteau et al. 1992; Dutrey et al. 1997) and NGC 2024-FIR5 (Richer et al. 1989, 1992). In L1448, a spectacular SiO jet is seen emanating from the driving source, aligned with the large-scale CO flow and unresolved across its width. In the NGC 2024-FIR5 flow, the fastest gas is seen to form an elongated jetlike feature on the axis of nested shells of lower-velocity gas. The collimation ratio q, defined as the width of the flow to the distance to the driving source, is as high as 30 for the high-velocity (30 km s^{-1}) gas in this source, but only 4 or so for the lower-velocity (5 km s^{-1}) envelope. Many other flows are now known that show this structure, with high-velocity elongated components tracing jetlike activity lying inside cavities of lower-velocity gas; examples include L1157 (Gueth et al. 1996), HH 111 (Cernicharo and Reipurth 1996; Nagar et al. 1997), and HH 211 (Gueth and Guilloteau 1999). All of these flows appear to be driven by very young, low-mass objects, based on their low luminosities and nondetection at even infrared wavelengths. The CO flow from HH 211 (Fig. 1) is perhaps the most striking image to date of this phenomenon, showing an unresolved CO jet with high-velocity gas ($v > 10$ km s^{-1} with no correction for inclination) lying within an ovoid cavity of slower-moving gas (<10 km s^{-1}). HH 211 is probably also one of the youngest low-mass outflows known, having a dynamical age $\tau_d = 0.07$ pc/10 km s^{-1} = 7000 years; if the source is inclined close to the plane of the sky, as is expected given the clear separation of red and blue outflow lobes and the relatively modest projected flow speeds, the true dynamical age could well be a factor of 5 or so lower. It appears that HH 211 is at the very start of its main accretion phase, and this perhaps explains

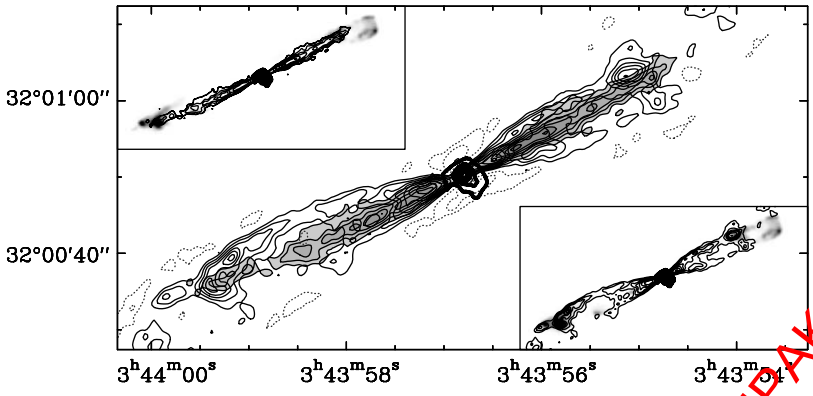

Figure 1. The HH 211 molecular jet mapped with the Plateau de Bure interferometer. The main panel shows the high-velocity CO jet in gray scale superposed on the lower-velocity outflowing gas, which forms a cavity around the jet. The thick contours show the 1.3-mm continuum emission. The panels top left and lower right show the fast and slow CO emission overlaid on the shocked H_2 line emission. Data taken from McCaughrean et al. (1994) and Gueth and Guilloteau (1999).

the relative simplicity of the outflow structure. Note that the full opening angle at the base of the flow is only 22°.

It is natural to identify these so-called "molecular jets" as the deeply embedded counterparts of the Herbig-Haro (HH) jets seen in less obscured systems and as the neutral counterparts of the ionized jets seen in the radio (see the chapters by Eislöffel et al. and by Hartigan et al., this volume). Important work by Raga (1991) and Hartigan et al. (1994) demonstrated that HH jets were denser and hence more powerful than initial estimates suggested (e.g., Mundt et al. 1987), so that the total momentum flux in HH jets integrated over the lifetime of a typical source is sufficient to drive the observed CO flows (e.g., Richer et al. 1992; Mitchell et al. 1994). This unified picture of jet-driven outflows is entirely consistent with the observed CO structures discussed above (Masson and Chernin 1993; Cabrit et al. 1997; Smith et al. 1997; Gueth and Guilloteau 1999). However, we caution that the actual composition of the driving jet, whether primarily atomic or molecular, is unknown. It is still unclear whether the CO jets seen in sources such as HH 211 and NGC 2024-FIR5 arise (1) from the body of a jet, where molecules have formed in the gas phase (Glassgold et al. 1989; Smith et al. 1997); (2) from molecules formed in the postshock region of shocks in the jet; or (3) from ambient molecular gas turbulently entrained along the jet's edge and at internal working surfaces (Raga et al. 1993; Taylor and Raga 1995).

RNO 43-FIR is another low-luminosity outflow source and is probably a flow in middle age (Bence et al. 1996; Cabrit et al. 1988): the driving source, with $L_\star = 6\ L_\odot$, is a heavily embedded Class 0 protostar invisible even at 2 μm, but the flow extends over a total size of 3 pc. The

outflow axis is close to the plane of the sky, so the image of CO integrated intensity shown in Fig. 2 shows both blue- and redshifted sides of the flow. The dynamical age is $\tau_d \sim 1.5\,\mathrm{pc}/10\,\mathrm{km\ s^{-1}} = 1.5 \times 10^5$ years, which is an upper limit, because of the small but unknown inclination angle. The CO flow is much more complex than in HH 211, and this most likely reflects the clumpy nature of the molecular gas through which the driving jet has passed; nonetheless, a very approximate S-shape

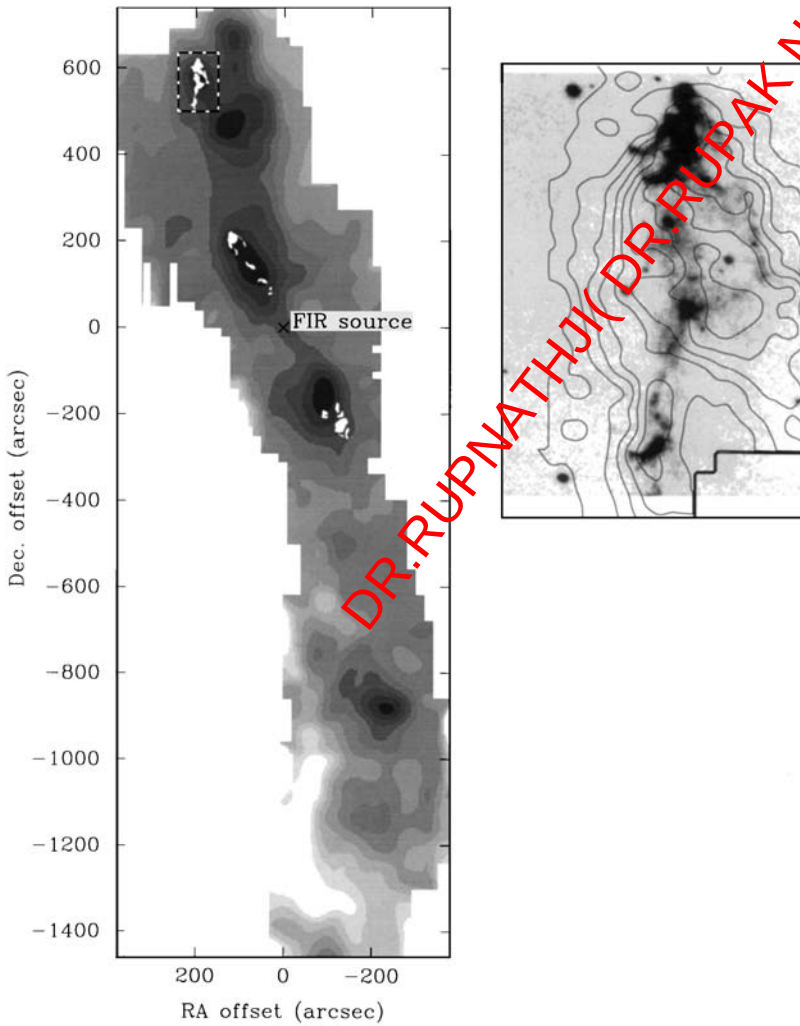

Figure 2. CO 2–1 image (in gray scale) of the RNO 43 molecular outflow (Bence et al. 1996); the driving far-IR (FIR) source is at the origin, marked with a cross. The solid white patches show the extent of the Hα emission. Note the large flow extent and correlation of the Hα emission with the CO hot spots. The panel to the right shows a detail from the northernmost Hα emission patch, showing the bow shock-shaped Hα structure in gray scale, and CO 2–1 contours overlaid.

symmetry can be seen about the driving source, both in the spatial and velocity data, suggesting that the jet direction has changed over time (Bence et al. 1996). A precessing-jet model, with a full cone angle of 27° and a precession timescale of order 3×10^4 years, provides a reasonable description of the overall flow properties (Bence et al. 1996); such precession could be driven by a binary companion in an inclined orbit.

The evidence that this flow is jet-driven, even at a distance of 1.5 pc from the driving source, is demonstrated by the Hα images of the object, which show strong emission coincident with the brightest CO points (see Fig. 2). In addition, at the northernmost CO feature in the flow, bright Hα coincident with a bow shock-shaped CO feature suggests that the whole of the RNO 43 outflow can be explained by the gradual sweeping up of a clumpy molecular cloud by a powerful stellar jet whose ejection axis varies slowly with time. It is also interesting to note that parsec-scale flows such as RNO 43 are the natural counterparts to the parsec-scale Herbig-Haro flows (Reipurth et al. 1997) seen in wide-field optical imaging. If there is molecular gas in the jet's path, then flows such as RNO 43 result, whereas jets in essentially empty space such as HH 34 (Devine et al. 1997) show only optical emission. This points strongly to the jets being primarily atomic in composition. However, in the HH 111 outflow system, CO "bullets" associated with the optical jet and having similar velocities to the optical gas have been detected far beyond the molecular cloud boundary (Cernicharo and Reipurth 1996). This suggests that, in some cases, the jets may have a molecular component.

Not all low-mass flows are jet-dominated. Many of the older flows show CO emission dominated by low-velocity cavities with little evidence for elongated high-velocity CO jet features. Examples include L43 (Bence et al. 1998), L1551 (Moriarty-Schieven and Snell 1988), and B5 (Velusamy and Langer 1998). These flows are typically 10^{5-6} years old and associated with nebulosities visible in the optical or at 2 μm, suggesting that they are Class I or II protostars, older than the Class 0 objects responsible for the HH 211, RNO 43, and NGC 2024-FIR5 outflows. The lack of high-velocity CO and obvious jetlike features in these flows (in contrast to their younger counterparts such as HH 211), as well as the presence of much wider cavities at the base of the flows, suggest that the jet power has declined over time and that a wider-opening-angle wind is now primarily responsible for driving the outflow. However, even in these older sources there is usually some evidence for weak jet activity. L1551 has an optical jet and extended Herbig-Haro emission, apparently, on one of its cavity walls (Davis et al. 1995; Fridlund and Liseau 1998), as well as fast CO emission suggestive of a jet origin (Bachiller et al. 1994), and B5 has optical jets stretching 2.2 pc away from the driving source. However, the L43 flow shows no signs of shocks, jets, or very fast CO, and this may be a true "coasting" flow, which is no longer being accelerated by a stellar wind or jet.

The recent interferometric images of the B5 outflow (Velusamy and Langer 1998) reveal a beautiful example of wide, hollow cavities at the base of the outflow, much like the reflection nebulosities seen in the near infrared in many of these systems; in order to reproduce the clearly separated red- and blueshifted emission lobes, the CO must be flowing along these cavity walls, presumably being accelerated by a poorly collimated radial wind from the star. The entire outflow driven by B5 has a dynamical age of 10^6 years and a collimation factor of about 5. The cavity opening angle at the protostar is extremely large, in the range 90–125°, and Velusamy and Langer (1998) suggest that if this angle further broadens with time, it may ultimately cut off the accretion flow. This idea is consistent with most of the available data: The young flows such as HH 211, RNO 43, and L1157 have opening angles less than 30° or so, whereas the older flows such as L1551, L43, and B5 are significantly greater than 90°. With maps at good resolution of a larger sample of outflows, it will be possible to test the hypothesis that flow opening angle is a measure of the source age.

B. High-mass Systems

Our understanding of massive flows is beginning to change, because we are starting to find a few isolated systems that can be studied in depth. However, we are still observationally biased toward older flows, which are easier to identify and study. This bias is likely to diminish in the future as more massive young flows are identified (e.g., Cesaroni et al. 1997; Molinari et al. 1998*a*; Zhang et al. 1998).

Most luminous YSOs have relatively wide-opening-angle outflows as defined by their CO morphology. Although the statistics are poor, because few massive flows have been studied with sufficient resolution to determine the morphology adequately, collimation factors q for seven well-mapped flows produced by YSOs with $L_{\rm bol} > 10^3$ $L_\odot$ range from 1 to 1.8 (NGC 7538 IRS1: Kameya et al. 1989; HH 80–81: Yamashita et al. 1989; NGC 7538 IRS9: Mitchell et al. 1991; GL 490: Mitchell et al. 1995; Ori A: Chernin and Wright 1996; W75N: Davis et al. 1998; G192.16: Shepherd et al. 1998). The dynamical timescales for these outflows range from 750 years to $\sim 2 \times 10^5$ years, and there is no obvious dependence of flow collimation on age. In comparison, collimation factors in low-mass outflows range from ~ 1 to as high as 10, with a typical value being ~ 2 or 3 (Fukui et al. 1993 and references therein). It appears that more luminous YSOs do not in general produce very well-collimated CO outflows, and this result is independent of outflow age, unlike outflows produced by low-luminosity YSOs. This may be because outflows from luminous YSOs tend to break free of their molecular cloud core at a very early stage in the outflow process. Hence, massive molecular flows are frequently the truncated base of a much larger outflow that extends well beyond the cloud boundaries (e.g., HH 80–81: Yamashita et al. 1989; DR21: Russell et al. 1992; G192.16: Devine et al. 1999).

The outflow from Orion A is perhaps the best-known and best-studied high-mass outflow system. The driving source is believed to be an O star, and the estimated age of the flow is ~750 years, which makes this one of the youngest known outflows. The flow differs significantly from those produced by low-luminosity sources and represents a spectacular example of the outflow phenomenon. The CO outflow is poorly collimated at all velocities and spatial resolutions, and the H_2 emission is dispersed into a broad fan shape that is unlike any other known outflow. Its morphology is highly suggestive of an almost isotropic, explosive origin. McCaughrean and Mac Low (1997) model the H_2 bullets as a fragmented stellar wind bubble using the fragmentation model of Stone et al. (1995) and suggest that the bullets are caused by several young sources within the BN-KL cluster. Chernin and Wright (1996) argue that the flow is driven by a single massive YSO, source I. The estimated opening angle, corrected for inclination, is approximately 60° for the blue lobe and 120° for the red lobe.

The outflow from G192.16 is perhaps more typical of outflows from B stars. Figure 3 shows an interferometric CO $J = 1$–0 image of the outflow together with a closeup of the 3-mm continuum emission showing a flattened distribution of hot dust (Shepherd et al. 1998; Shepherd and Kurtz 1999). The 3-pc-long molecular flow represents the truncated base of a much larger flow, identified by Hα and [S II] emission, that extends almost 5 pc from the YSO (Devine et al. 1999). The CO flow is ~10^5 years old and appears to be driven by an early B star. Despite the very different masses and energies involved, the CO morphology looks very similar to

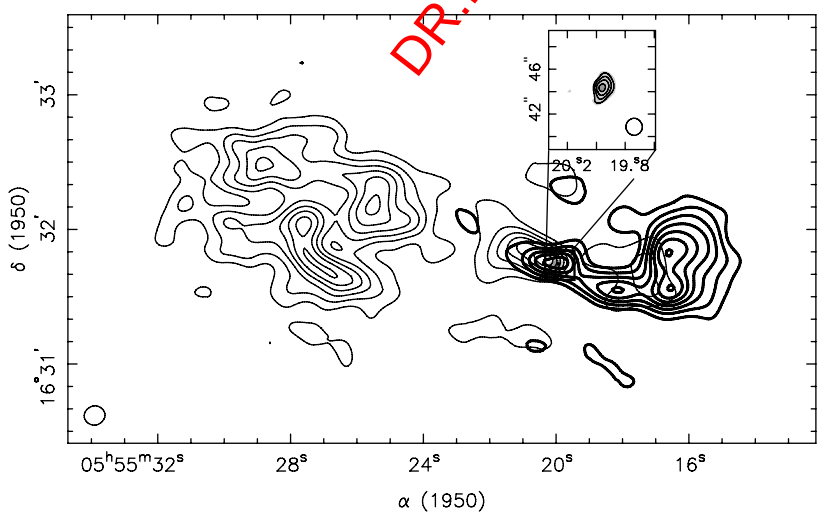

Figure 3. The G192.16 outflow mapped with the Owens Valley Radio Observatory (OVRO) interferometer. Contours of redshifted CO (thick lines) and blueshifted CO (thin lines) delineate the bipolar flow emanating from a dense core, traced by the central dust continuum emission represented in gray scale.

L1551-IRS5: the extent of the G192.16 CO outflow is 2.6×0.8 pc, approximately twice that of L1551, but the mass in the outflow (≈ 95 $M_\odot$) is much greater. The opening angle at the base of the flow is $\sim 90°$.

The present lack of well-collimated CO outflows with $q > 3$ from YSOs with $L_{bol} > 10^3$ $L_\odot$ does not mean that jets and well-collimated structures are not present in these massive sources. For example, the central source in HH 80–81 ($L_{bol} \sim 2 \times 10^4$ $L_\odot$) powers the largest known Herbig-Haro jet, with a total projected length of 5.3 pc, assuming a distance of 1.7 kpc (Martí et al. 1993, 1995 and references therein). However, the CO flow appears poorly collimated, with $q \sim 1$ when mapped at moderate resolution (Yamashita et al. 1989). Also, the biconical thermal radio jet from Cepheus A HW2 ($L_{bol} \sim 10^4$ $L_\odot$) appears to be responsible for at least part of the complicated molecular flow seen in CO and shock-enhanced species such as H_2, SiO, and SO (e.g., Doyon and Nadeau 1988; Martín-Pintado et al. 1992; Hughes 1993; Torrelles et al. 1993; Rodríguez et al. 1994; Rodríguez 1995; Garay et al. 1996; Hartigan et al. 1996; Narayanan and Walker 1996). The HH 80–81 and Cepheus A HW2 systems demonstrate that high-luminosity YSOs can produce well-collimated jets like those found in association with less luminous stars, even though the CO flow may appear chaotic or poorly collimated. Other examples of possible jets in massive outflows include IRAS 20126 and W75N IRS1. IRAS 20126 ($L_{bol} \sim 1.3 \times 10^4$ $L_\odot$) appears to drive a compact jet seen in SiO and H_2 (Cesaroni et al. 1997). W75N IRS1 ($L_{bol} \sim 1.4 \times 10^5$ $L_\odot$) shows H_2 2.12-μm shock-excited emission at the end and sides of the CO lobe, with a morphology and emission characteristics highly suggestive of a jet bow shock (Davis et al. 1998). However, this "bow shock" is 0.3 pc wide, i.e. 30 times larger than the H_2 2.12-μm bow shock at the end of the HH 211 flow (cf. Fig. 1). It is not fully clear whether such wide bows are created by protostellar jets or by a low-collimation wind component. Scaling up from current hydrodynamical jet simulations (e.g. Suttner et al. 1997), one would need a jet radius of ~ 0.03 pc at 1.3 pc from the star, hence a jet opening angle $\sim 2.6°$.

C. Outflow Velocity Structure

From the above discussion, we conclude that jet activity, bow shocks, and CO cavities are common to outflows from low- and high-mass systems. There is some evidence that high-mass systems are less well collimated than low-mass ones, but that may be due to selection effects: Young, high-mass systems with small opening angles may simply be missing from the small sample currently known (although the Orion outflow does appear to be very young). This conclusion suggests it is sensible to consider the possibility that a common driving mechanism is responsible for all outflows.

Several authors have noted that molecular flows seem to be characterized by a power law dependence of flow mass $M_{CO}(v)$ as a function of velocity. The power law exponent γ (where $M_{CO}(v) \propto v^\gamma$) is typically ~ -1.8 for most low-mass outflows, although the slope often steepens at

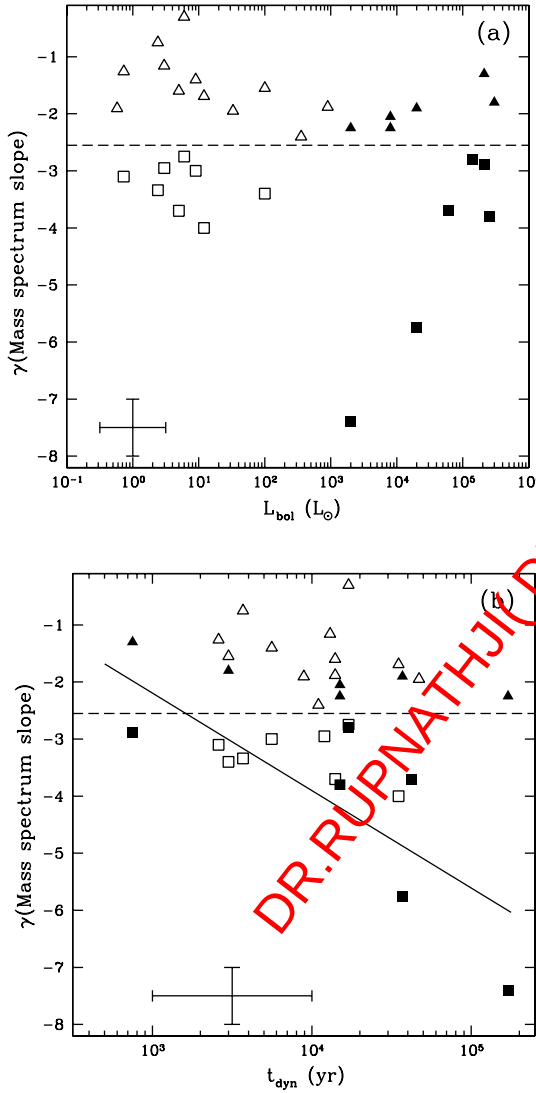

Figure 4. The slope γ of the mass spectrum $M(v)$ plotted as a function of (a) source bolometric luminosity and (b) flow dynamical age τ_d. Triangles represent γ for gas with projected speeds less than 10 km s^{-1} relative to the source, and squares are for gas moving at more than 10 km s^{-1}. The dashed, horizontal line separates the low- and high-velocity γ's for clarity. Sources with $L_{bol} < 10^3$ L$_\odot$ are plotted with open symbols, those with $L_{bol} > 10^3$ L$_\odot$ with filled symbols. Representative error bars are displayed in the lower left corner of each plot. The solid line in part (b) is a linear least-squares fit (slope -1.7 ± 0.6) to high-velocity γ's in luminous sources vs. log(τ_d). The sources plotted here are VLA 1623, IRAS 03282, L1448-C, L1551-IRS5, NGC 2071-IRS1, and Ori A IRC2 (Cabrit and Bertout 1992); TMC-1 and TMC-1A (Chandler et al. 1996); L379-IRS1-S (Kelly and MacDonald 1996); NGC 2264G (Lada and Fich 1996); G5.89-0.39 (Acord et al. 1997). Cep E (Smith et al. 1997) HH 251-254, NGC 7538-IRS9, W75N-IRS1, and NGC 7538-IRS1 (Davis et al. 1998); G192.16 (Shepherd et al. 1998); and HH 26IR, LBS 17-H, G35.2-0.74, HH 25MMS (A. Gibb, personal communication).

velocities greater than 10 km s^{-1} from v_{LSR} (e.g., Masson and Chernin 1992; Rodríguez et al. 1982; Stahler 1994; Chandler et al. 1996; Lada and Fich 1996; A. Gibb, personal communication).

Figure 4 plots (a) γ vs. L_{bol} and (b) γ vs. the dynamical timescale t_{dyn} for a new compilation of 22 sources with luminosities ranging from 0.58 $L_\odot$ to 3×10^5 $L_\odot$. Triangles represent slopes derived from gas moving less than 10 km s^{-1} relative to v_{LSR} while squares represent slopes derived from gas moving more than 10 km s^{-1} relative to v_{LSR}. Sources with $L_{bol} < 10^3$ $L_\odot$ are plotted with open symbols, while those with $L_{bol} > 10^3$ $L_\odot$ are plotted with filled symbols. Both well-collimated and poorly collimated outflows are represented in the sample.

The most striking result from Fig. 4a is that γ's for low-velocity gas are similar in sources of all luminosities. This suggests that a common gas acceleration mechanism may operate over nearly six decades in L_{bol}. In addition, there is a clear separation between γ's in high- and low-velocity gas, which supports the interpretation that there are often two distinct outflow velocity components, perhaps corresponding to a recently accelerated component and a slower, coasting component.

Hydrodynamic simulations of jet-driven outflows from low-luminosity YSOs predict such a change of slope at high velocity. They also predict that γ should steepen over time, possibly due to the collection of a reservoir of low-velocity gas (Smith et al. 1997). Figure 4b reveals marginal evidence that the mass spectrum in flows from luminous YSOs does become steeper with time, in both the low- and high-velocity ranges. The solid line in Fig. 4b is a linear least-squares fit (slope -1.7 ± 0.6) to high-velocity γ's in luminous sources versus $\log(\tau_d)$. There is no indication of time evolution of the mass spectrum slopes in outflows from low-luminosity sources.

The decrease of γ with time in more luminous sources may be due to a difference in the driving mechanism, or it may simply be more prominent because the mass outflow rate is several orders of magnitude greater than in outflows from low-luminosity YSOs (thus allowing more precise determination of γ) and because their flow ages cover a broader range, from 750 to 2×10^5 yrs.

III. TESTS OF PROTOSTELLAR WIND AND ACCRETION MODELS

A. Flow Energetics

It is well known that outflow energetics correlate reasonably well with L_{bol} over the entire observed luminosity range. In Fig. 5a, we show a recent compilation of the mean momentum deposition rate F_{CO} as a function of bolometric luminosity of the driving star. It must be remembered that F_{CO} is the time-averaged force required to drive the CO outflow: $F_{CO} = M_{CO}\, v_{CO}/\tau_d$, where we assume that τ_d is a good approximation

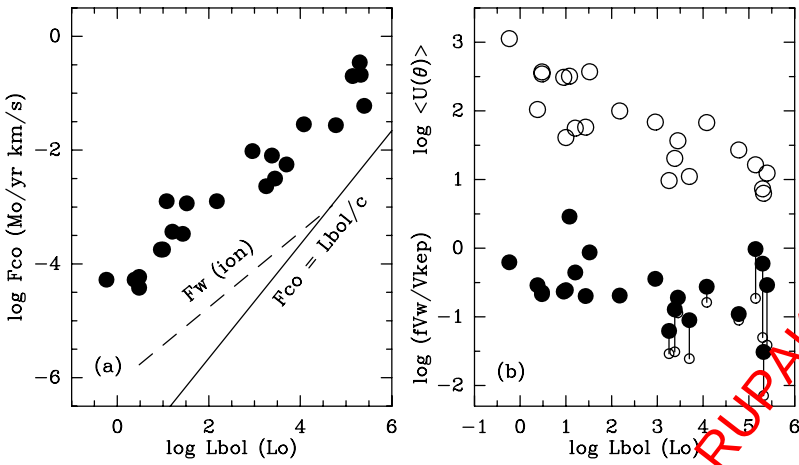

Figure 5. (a) Average momentum flux in the CO flows as a function of source luminosity. The solid line shows the force available in stellar photons (assuming single scattering), and the dashed line the force available from the ionized wind components (data from Panagia 1991). (b) The factor fv_w/v_K derived for the same set of sources is plotted as solid circles (small open circles assume that luminous sources are on the zero-age main sequence). Large open circles show the required $\langle U(\theta)\rangle$ factors for the same objects if the circulation models are applicable (see text for details).

to the flow age. If the CO-emitting material is accelerated by a separate stellar wind (or jet), the wind momentum flux F_w may be quite different from F_{CO}, depending on the nature of the wind-cloud interaction. There are clearly large uncertainties in the measured flow properties, primarily due to difficulties in estimating the inclination angle of the outflow, the optical depth and excitation of the CO, and the correctness of the assumption that the dynamical timescale is a good estimate of the flow age (Cabrit and Bertout 1992; Padman et al. 1997). However, as seen in Fig. 5a, the correlations are roughly consistent with a single power law (here of slope ~ 0.7) across the full range of source luminosities. It has been suggested that this correlation argues for a common entrainment or driving mechanism for molecular flows of all masses; but this is by no means a compelling argument, given that we would surely expect most physically reasonable outflow mechanisms to generate more powerful winds if the source mass and luminosity are increased.

Regardless of the details of how the stellar wind or jet entrains material, if the shock cooling times are short compared to flow dynamical timescales (as we expect for wind speeds less than 300 km s^{-1}; Dyson 1984, or if there is efficient mixing at the wind/molecular gas interface; Shu et al. 1991), then the wind and molecular flow momenta will be equal. This is often called the momentum-conserving limit. Then molecular outflows represent a good opportunity to test proposed protostellar ejection

mechanisms. In particular, we show in this section that they can be used to estimate the ratio f of ejection to accretion rates that would be necessary if the wind is accretion-powered.

We first recall that optically thin, line-driven radiative winds (such as those present in main-sequence O and B stars) are insufficient to drive the flows if the flows are momentum-driven. The solid line in Fig. 5a shows the maximum momentum flux available in stellar photons in the single-scattering limit, $L_{\rm bol}/c$. It falls short of the observed amount in molecular flows by one to three orders of magnitude. If flow lifetimes have been underestimated, the discrepancy is reduced, but not by a sufficient amount. In principle, higher momentum flux rates could be reached with multiple scattering. Wolf-Rayet stars ($L_{\rm bol} \sim$ a few 10^5 $L_\odot$) have a wind force reaching 20–50$L_{\rm bol}/c$, similar to the momentum rate in molecular flows from sources of comparable luminosity (cf. Fig. 5a). Such high values are attributed to multiple scattering of each photon by many lines closely spaced in frequency (e.g., Gayley et al. 1995 and references therein). However, excitation conditions in protostellar winds are very different from those in hot, ionized Wolf-Rayet winds. The dashed line in Fig. 5a shows the typical momentum flux in the ionized component of protostellar winds, inferred from recombination lines or radio continuum data (Panagia 1991): the values lie a factor of 10 below F_{CO}, implying that the driving winds must be 90% neutral. If dust grains instead provide the dominant opacity source in protostellar winds, comparison with winds from cool giants and supergiants might be more appropriate. Their wind velocities are $\simeq$5–30 km s^{-1}, and mass loss rates do not exceed 10^{-4} $M_\odot$ yr^{-1}, hence $F_w \leq 0.5 - 3L_{\rm bol}/c$ for a typical $L_{\rm bol} \sim 5 \times 10^4$ $L_\odot$. Calculations by Netzer and Elitzur (1993) show that 10 times larger mass loss rates could in principle be achieved in oxygen-rich stars, where silicates dominate the opacity curve. The wind force could then become comparable to the molecular outflow momentum rate for $L_{\rm bol} \sim 5 \times 10^4$ $L_\odot$. Hence, it is just possible that luminous stars ($L_\star > 5 \times 10^4$ $L_\odot$) could drive their flows by radiative acceleration if dust opacity plays a significant role; further work is needed to investigate whether such models are viable. In lower-luminosity sources, however, the opacity required to lift material above escape speeds largely exceeds typical values for circumstellar dust. Therefore, molecular outflow sources with $L_\star < 5 \times 10^4$ $L_\odot$ must possess an efficient nonradiative outward momentum source.

It thus appears most likely that both low- and high-mass systems possess an efficient nonradiative wind generation mechanism in their embedded protostellar phase. If energetic bipolar winds are the chief means of angular momentum loss during the main accretion phase for stars of all mass, this is not surprising. However, the details of the wind ejection mechanism could differ; in particular, massive accreting stars are likely to have thinner convective layers and probably rotate faster, so that the magnetic field and accretion geometry close to the star may be very different from those in low-mass stars.

There exist quite a number of efficient accretion-powered wind mechanisms from the stellar surface, disk, or disk-magnetosphere boundary. The most efficient models use a strong magnetic field in the star or disk to drive the wind and to carry off angular momentum from the accreting gas (e.g., see reviews by Königl and Pudritz and by Shu et al., this volume). This wind is further collimated by magnetic or hydrodynamic processes (e.g., Mellema and Frank 1997), generating a high-Mach number wind or jet with a speed of order 200–800 km s^{-1}. A fraction $f < 1$ of the accretion flow $\dot{M}_a$ is ejected in the wind: $\dot{M}_w = f\,\dot{M}_a$.

A different scenario recently explored by Fiege and Henriksen (1996*a, b*) is that molecular flows are not predominantly swept up by an underlying wind but represent infalling gas that has been deflected into polar streams by magnetic forces. Only a small fraction of the infalling gas actually reaches the star to produce accretion luminosity. In that case, $f > 1$. This model has been invoked in particular to explain the large flow masses $M_{\rm CO} \sim 10 M_\star$ observed in flows from luminous sources. In the following we use molecular flow observations to set constraints on these two classes of proposed models.

B. The Ejection/Accretion Ratio in Protostellar Winds

Two simple, independent methods have been used in the literature to estimate f, assuming that the driving mechanism is steady over the source lifetime. First, in low-mass protostars where the luminosity is accretion-dominated, it is possible to use the observed correlation of flow force with $L_{\rm bol}$ (Fig. 5a) to derive the ejection fraction f. The source bolometric luminosity is $L_{\rm bol} = GM_\star \dot{M}_a / R_\star = \dot{M}_a\, v_K^2$, where v_K is the Keplerian speed at the stellar surface. The flow and wind force (assuming momentum conservation) is $F_{\rm CO} = f\,\dot{M}_a\, v_w$. Hence $F_{\rm CO}/L_{\rm bol} = f\, v_w / v_K^2$. A value $f \sim 0.1$ is inferred in both Class 0 and Class I low-luminosity objects (Bontemps et al. 1996). Alternatively, if one estimates $M_\star$ from $L_{\rm bol}$ via the zero-age main-sequence (ZAMS) relationship (which is probably valid only for sources with $L_{\rm bol} > 10^3$ L$_\odot$), one can use the accumulated flow momentum to infer f, using: $P_{\rm CO} = v_w\, M_w = f\, M_\star\, v_w$. Values of f ranging from 0.1 to 1 are inferred for a wind speed of 150 km s^{-1} (Masson and Chernin 1994; Shepherd and Churchwell 1996). However, we point out that wind speeds are unlikely to remain constant over the whole $L_{\rm bol}$ range. There is evidence for higher wind velocities in luminous flow sources: for example, proper motions up to 1400 km s^{-1} are seen in HH 80–81 (Martí et al. 1995), and Z Canis Majoris shows optical jet emission with speeds up to 650 km s^{-1} (Poetzel et al. 1989). These are significantly higher than the 100–200 km s^{-1} typically seen in low-mass sources.

To reexamine this issue in a homogeneous way over the whole luminosity range, we plot in Fig. 5b the values of $f v_w / v_K$ obtained using a new combination of the above two methods (Cabrit and Shepherd, in preparation). The solid circles are derived assuming the luminosity is accretion-dominated, whereas the open circles (for sources more lumi-

nous than 10^3 $L_\odot$) assume the ZAMS relationship given above. Typically, v_K ranges from 100 km s^{-1} in low-luminosity sources to 800 km s^{-1} in high-luminosity sources. A rather constant value $fv_w/v_K \sim 0.3$ seems to hold over the whole range of $L_{\rm bol}$. This value is in line with both popular magnetohydrodynamic (MHD) ejection models. In the x-wind model (Shu et al. 1994, and chapter in this volume), the wind is launched close to the stellar surface ($v_w \sim v_K$), and a large fraction of the accreting gas is ejected ($f \sim 0.3$). In the self-similar disk-wind models (Ferreira 1997; see the chapter by Königl and Pudritz, this volume), less material is ejected ($f \sim 0.03$), but the long magnetic lever arm accelerates it to many times the Keplerian speed ($v_w \sim 10v_K$). Thus we conclude that the energetics of the flows over the entire luminosity range are broadly consistent with a unified MHD ejection model for all flow luminosities, but we reiterate that given the very different physics involved around high- and low-mass protostars, the details of such a model for high-mass systems are still unclear.

We stress again that this plot assumes perfect momentum conservation in the wind/flow interaction. There could be strong deviations from this key assumption. First, we should keep in mind the possibility that massive flows enter the energy-driven regime: for high wind speeds, the gas cooling behind the shock will be slow, and the snowplow or momentum-conserving flow will turn into an energy-driven one. In that case, the shell momentum can exceed the momentum in the wind itself by a factor of order $v_w/v_{\rm CO}$ (Cabrit and Bertout 1992; Dyson 1984), so reducing markedly the momentum requirement of the driving wind. Of course, there are objections to energy-driven flows, in particular their inability to reproduce the bipolar velocity fields of many flows (Masson and Chernin 1992); but given the apparently poorer collimation of high-mass outflows, this issue should perhaps be reexamined. Second, if the flow is entrained in a jet bow shock, the efficiency of momentum transfer will depend on the ratio of ambient to jet density: it will be close to 1 only if the jet is less dense than the ambient medium. Highly overdense jets will pierce through the cloud without depositing much of their momentum (Chernin et al. 1994), and in that case the ratio fv_w/v_K plotted in Fig. 5b would have to be increased. We conclude that for current protostellar jet models to apply, we have the additional condition that most of the jet momentum must be in a component that is not significantly denser than the ambient molecular cloud on scales of 0.1–1 pc.

The foregoing analysis also provides important constraints on accretion rates in protostellar objects of various masses. If $fv_w/v_K \sim 0.3$, then the values of $F_{\rm CO}$ in Fig. 5a show that $\dot{M}_a = 3F_{\rm CO}/v_K$ must range from a few 10^{-6} $M_\odot$ yr^{-1} at $L_{\rm bol} \sim 1$ $L_\odot$ to a few 10^{-3} $M_\odot$ yr^{-1} at $L_{\rm bol} \sim 10^5$ $L_\odot$. Then protostellar sources would not be characterized by a single infall rate across the whole stellar mass range, and massive stars would form with much higher infall rates than low-mass stars (Cabrit and Shepherd, in preparation).

The wealth of data available on low-mass systems also allows one to break the samples down by estimated age, and so look for evolution of outflow properties with stellar age. Bontemps et al. (1996) made an important study of low-mass systems in Taurus and Ophiuchus and found evidence for a secular decline in outflow power with age, while f remained constant. Intriguingly, the best correlation of outflow power was with circumstellar mass (as measured by the millimeter continuum flux) rather than with source bolometric luminosity; Saraceno et al. (1996) also presented a similar correlation between millimeter continuum flux and outflow kinetic luminosity in systems with $L < 10^3\ L_\odot$. These results strongly suggest that the accretion rate and the outflow strength both decline in proportion to the disk and envelope mass.

C. Deflected Infall Models

Although the above analysis shows that f need not be necessarily higher in high-mass outflows, the very large masses involved, combined with the inefficiency of entrainment and momentum transfer by dense jets (especially once they escape their parent clouds), has led to some discussion of whether the sweeping up of ambient molecular gas by an accretion-driven wind is a viable mechanism for these objects (e.g., Churchwell 1997).

A recent class of outflow models, termed circulation models, can naturally generate outflow masses much greater than the stellar mass. In these, most of the infalling circumstellar material is diverted magnetically at large radii into a slow-moving outflow along the polar direction, while infall proceeds along the equatorial plane (Fiege and Henriksen 1996*a*,*b*). The main attraction of these models is that they generate large outflow masses for even small stellar masses and can generally explain the observed opening angles and velocity structures seen in high-mass systems. In particular, self-similar models predict that the velocity and density laws should take the form $V(r,\theta) = U(\theta)\sqrt{GM_\star/r}$ and $\rho(r,\theta) = \mu(\theta)M_\star r_0^{-3}(r/r_0)^{2\alpha-0.5}$, where $0.25 \geq \alpha > -0.5$, r_0 is an unspecified radial scale, and $U(\theta)$ and $\mu(\theta)$ are dimensionless functions. It is then straightforward to show that the force and ~~mass~~ flux in the outflow are related by $F_{\rm CO}/\dot{M}_{\rm CO} = \sqrt{GM_\star/R_{\rm CO}}\langle U(\theta)\rangle$ where $\langle U(\theta)\rangle = \int U(\theta)^2\mu(\theta)d\omega / \int U(\theta)\mu(\theta)d\omega$ is the density-weighted average velocity over the outflow solid angle. The inferred $\langle U(\theta)\rangle$ (using the same $M_\star$ as for our estimates of $f\,v_w/v_K$) is ~~plotted in~~ the top part of Fig. 5b as open circles. It is clear that high values (between 1000 and 10) are required. Generalized circulation models that include Poynting flux driving yield values of $\langle U(\theta)\rangle$ between 5 and 200 (Lery et al., in preparation). In model cases in which radiation transport is important in setting up the flow, a power law slope of 0.8 is predicted between $F_{\rm CO}$ and $L_{\rm bol}$, which is close to the observed slope ~ 0.7 (see also Henriksen 1994). Observations seem to indicate a systematic decline of $\langle U(\theta)\rangle$ with $L_{\rm bol}$, which would also have to be explained.

There are several concerns about these circulation models. First, there are many unipolar CO outflows known, such as NGC 2024-FIR5 (Richer et al. 1992), and the almost-unipolar HH 46–47 system (Chernin and Masson 1991). These are naturally explained by swept-up wind models if the protostar is forming on the edge of a cloud or close to an H II region interface: the jet or wind propagating into the cloud will then sweep up a large CO flow, while in the opposite direction little evidence for a CO lobe will be seen. In circulation models, anisotropic solutions may also occur, but it is unclear why the weaker lobe would necessarily be on the side where the large-scale cloud density is low. Second, in some objects such as B5 (Velusamy and Langer 1998), there is an apparent lack of molecular material in the equatorial plane that can feed a circulation flow. Third, as discussed in section II, in some high-mass systems such as HH 80–81, there is direct evidence for fast jets and bow shock entrainment of molecular gas. Consequently, it seems more probable, given the evidence presented, that even high-mass outflows can be generated by the sweeping up of ambient cloud material by an accretion-driven stellar wind or jet. The details of the MHD driving mechanism in these cases, and of the momentum transfer between the wind and the jet, remain open issues.

IV. SHOCK CHEMISTRY AND ENERGETICS

The interaction between a supersonic protostellar wind and surrounding quiescent material is expected to drive strong shock fronts. Shocks can be of type C (continuous) or J (jump), depending on the shock velocity, the magnetic field, and the ionization fraction of the preshock gas (Draine and McKee 1993; Hollenbach 1997). In the last few years, spectacular gains in sensitivity in the millimeter and IR domains have allowed us for the first time to witness the chemical and thermal effects of these shocks in molecular outflows. These observations yield direct estimates of the flow age, energetics, and entrainment conditions, which represent an important new step toward a complete description of the outflow phenomenon.

A. Chemical Processing of ISM in Molecular Flows

1. Theoretical Expectations. By compressing and heating the gas, shock waves trigger new chemical processes, which lead to a specific "shock chemistry" (see the chapter by Langer et al., this volume). The most active molecular chemistry is expected to occur in C-shocks, because they increase the temperature to moderate values of about 2000 K in a thick layer, where molecules can survive and reactions that overcome energy barriers can proceed. In particular, the very reactive OH radical can be formed by $O + H_2 \rightarrow OH + H$ (which has an energy barrier of 3160 K) and will contribute to the formation of H_2O by further reaction with H_2: $OH + H_2 \rightarrow H_2O + H$ (energy barrier: 1660 K). In dissociative J-shocks, molecules are destroyed in the hot ($T \sim 10^5$ K) thin postshock layer and

reform only over longer timescales, in a plateau of gas at ~400 K. Since some of these chemical processes are fast, and the cooling times are short, the chemical composition of the shocked regions is expected to be strongly time dependent.

Shocks also process dust grains. In the most violent J-shocks, destruction of grain cores and thermal sputtering inject refractory elements (such as Si and Fe) into the gas phase (e.g., Flower et al. 1996). In slower C-type shocks, nonthermal sputtering will inject refractory and volatile species mainly from the grain mantles into the gas phase (e.g., Flower and Pineau des Forêts 1994). The entrance of this fresh material, together with the high abundance of OH, will produce oxides such as SO and SiO (see Bachiller 1996; van Dishoeck and Blake 1998; and references therein). As the shocked gas cools, the dominant reactions will again be those of the usual low-temperature chemistry, and depletion onto dust grain surfaces will reduce the abundances of some of the newly formed molecules (e.g., H_2O, see Bergin et al. 1998). However, the chemical composition of both the gas and the solid phases will remain altered with respect to preshock ones.

2. Observations. The chemical effects of shocks have been observed in numerous outflows from low-mass Class 0 objects, which are particularly energetic and contain shocked regions well separated spatially from the quiescent protostellar envelope. Recent examples include IRAS 16293 (Blake et al. 1994; van Dishoeck et al. 1995), NGC 1333 IRAS4 (Blake et al. 1995), and NGC 1333 IRAS2 (Langer et al. 1996; Blake 1997; Bachiller et al. 1998).

A comprehensive study of many different species has recently been carried out on L1157 (Bachiller and Pérez Gutiérrez 1997). The abundances of many molecules (e.g., CH_3OH, H_2CO, HCO^+, NH_3, HCN, HNC, CN, CS, SO, and SO_2) are observed to be enhanced by factors ranging from a few to a few hundred. The extreme case is SiO, which is enhanced by a factor of $\sim 10^6$. There are significant differences in spatial distribution among the different species: some molecules, such as HCO^+ and CN, peak close to the central source, whereas SO and SO_2 have a maximum in the more distant shocks, with OCS having the most distant peak. Other molecules, such as SiO, CS, CH_3OH, and H_2CO, show an intermediate behavior. Such differences cannot be attributed solely to excitation conditions; an important gradient in chemical composition is observed along the outflow. It is very likely that this strong gradient is related to the time dependence of shock chemistry. As an example, consider the chemistry of SO, SO_2, and OCS, which has been recently modeled by Charnley (1997). It is believed that sulfur is released from grains in the form of H_2S and that it is then oxidized to SO and SO_2 in a few 10^3 yr. The formation of OCS needs a few 10^4 yr. This is in general agreement with observations, because the SO/H_2S and SO_2/H_2S ratios do increase with distance from the source (i.e., with time), and OCS emission is only observed in the most distant position (i.e., the oldest shock). Hence, chem-

ical studies are of high potential to constrain the age and time evolution of molecular outflows.

B. Shock Cooling and Energetics

Millimeter observations of shock-enhanced molecules trace chemically processed gas that has already cooled down to 60–100 K, as indicated, e.g., by multiline NH_3 studies (Bachiller et al. 1993; Tafalla and Bachiller 1995). Emission from hotter postshock gas, on the other hand, is important to obtain information on the instantaneous energy input rate and preshock conditions in outflows.

1. Hot ($T \geq 1000$ K) Shocked Gas. Hollenbach (1985) suggested that the [O I] 63-μm line should offer a useful, extinction-insensitive measure of dissociative J-shocks in molecular flows. Because [O I] 63 μm is the main coolant below ~5000 K, its intensity is roughly proportional to the mass flux into the J-shock, $\dot{M}_{\rm JS}$, through the relation $L_{\rm [O\ I]}/L_\odot = 10^4 \times \dot{M}_{\rm JS}/M_\odot {\rm yr}^{-1}$, as long as the line remains optically thin (i.e., $n_0 V_{\rm JS} < 10^7$ km s^{-1} cm^{-3}, where n_0 is the preshock density and $V_{\rm JS}$ is the J-shock velocity).

First detections of [O I] 63 μm in outflows were obtained with the Kuiper Airborne Observatory (KAO) toward three HH objects and five highly collimated Class 0 outflows (Cohen et al. 1988; Ceccarelli et al. 1997). Since the advent of the *Infrared Space Observatory* (ISO), the Long Wavelength Spectrometer (LWS) has revealed [O I] 63-μm emission in at least 10 more HH objects and molecular outflows (Liseau et al. 1997; Saraceno et al. 1998). These authors find a surprisingly good correlation between *current* values of $\dot{M}_{\rm JS}$ derived from [O I] 63 μm and *time-averaged* $\dot{M}_{\rm ave}$ values derived from millimeter observations of the outflow, assuming ram pressure equilibrium at the shock (i.e., $F_{\rm CO} = \dot{M}_{\rm ave} \times V_{\rm JS}$). Both values agree for $V_{\rm JS} \sim 100$ km s^{-1}. The dispersion in this correlation, roughly a factor of 3, is of the same order as the uncertainties in $F_{\rm CO}$ caused by opacity and projection effects (Cabrit and Bertout 1992). Hence, CO-derived momentum rates in outflows do not appear to suffer from large systematic errors.

With the development of large-format near-IR arrays in the early 1990s, it also became possible to map molecular outflows in the 2.12-μm $v = 1$–0 S(1) line of H_2, a tracer of hot (~2000 K) shocked molecular gas. In both low-luminosity and high-luminosity outflows, the H_2 emission delineates single or multiple bow-shaped features associated with the leading edge of the CO emission (Davis and Eislöffel 1995; Davis et al. 1998), as illustrated in Fig. 1 for HH 211; in a few cases, H_2 emission also traces collimated jets and cavity walls (e.g., Bally et al. 1993; Eislöffel et al. 1994). Observed surface brightnesses and rotational temperatures ~1500–2500 K indicate moderate-velocity shocks, either J-shocks of speed 10–25 km s^{-1} or C-shocks with $v_s \sim 30$ km s^{-1} and low filling factor (Smith 1994; Gredel 1994). In particular, the morphology, line profile shapes, intensity, and proper motions of H_2 2.12-μm bows are

well reproduced by hydrodynamical simulations of jets propagating into the surrounding cloud, where H_2 2.12-μm emission arises mostly in the nondissociative wings of the bow shock (Raga et al. 1995; Micono et al. 1998; Suttner et al. 1997).

If these bow shocks are also where most of the slow molecular outflow is being accelerated, and if H_2 emission dominates the cooling (as expected, e.g., in 2000-K molecular gas at densities of 10^5–10^8 cm^{-3}), then $L(H_2)/L_{CO}$ should be of order unity (see, e.g., Hollenbach 1997). In the five flows studied by Davis and Eislöffel (1995), the observed ratio $L(H_2)/L_{CO}$ has a median value of ~0.4, but it covers a very broad range from 0.001 to 30. The discrepancies could be caused by uncertainties in 2-μm extinction (corrections typically amount to 10–100 for A_V = 20–50 mag); by the use of unreliable L_{CO} estimates; or, in the case of very low ratios, by a strong decrease in outflow power over time (W75N; see Davis et al. 1998). Hence the H_2 2.12-μm line alone is not a sufficient diagnostic of the outflow entrainment process.

2. Warm ($T \sim 300$–1000 K) molecular Gas. The ISO mission has led to the detection of a new component of warm postshock gas at $T \sim 300$–1000 K in several outflows. Figure 6 shows a map of the L1157 outflow in the $v = 0$–0 S(5) pure rotational line of H_2 at 6.9 μm, obtained with ISOCAM (Cabrit et al. 1998). A series of bright emission spots are seen along the outflow axis. They coincide spatially with hot shocked gas emitting in the H_2 2.12-μm line (Eislöffel and Davis 1995) and with the various peaks of shock-enhanced molecules identified by Bachiller and Pérez Gutiérrez (1997; see section IV.A). However, they trace an intermediate temperature regime of ~800 K, considerably lower than the 2000 K observed in rovibrational H_2 lines. Warm H_2 at 700–800 K was also found with the ISO Short Wavelength Spectrometer (SWS) in two outflows from very luminous sources, Cepheus A and DR 21 (Wright et al. 1996; Smith et al. 1998). Finally, warm CO at $T \sim 330$–1600 K was detected in high-J lines (J_{up} = 14 to 28) with ISO-LWS toward five outflows of various luminosities, and H_2O and OH lines were detected in two cases (Nisini et al. 1996, 1998; Ceccarelli et al. 1997).

The observed emission fluxes and temperatures in H_2 and CO are well explained by nondissociative J-shocks with $v_s \sim 10$ km s^{-1} or slow C-shocks with $v_s \sim 10$–25 km s^{-1}, and $n_0 \sim 10^4$–3×10^5 cm^{-3} (e.g., Wright et al. 1996; Nisini et al. 1998; Cabrit et al. 1998). One important constraint is the rather low $[H_2O]/[H_2]$ abundance ratio ~1–2 $\times$ 10^{-5} observed in HH54 and IRAS16293 (Liseau et al. 1997; Ceccarelli et al. 1997); steady-state C-shocks would predict complete conversion of O into water. The relatively high $[OH]/[H_2O]$ ratio $\sim \frac{1}{4}-\frac{1}{10}$ in these two flows suggests that the shock age is too short for conversion to be complete and points to the need for time-dependent C-shock models for proper interpretation of the data (e.g., Chièze et al. 1998).

Mid- and far-infrared emission from this warm molecular gas component appears more tightly correlated with L_{CO} than the 2-μm H_2 lines.

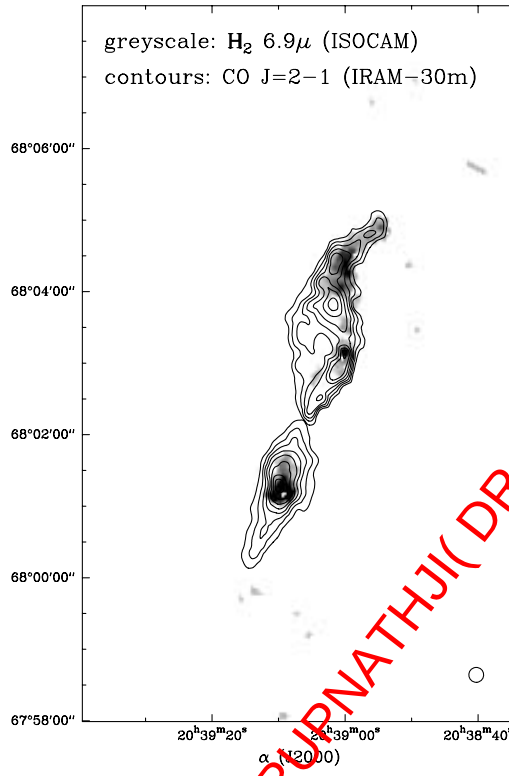

Figure 6. The L1157 outflow mapped in the 6.9-μm pure rotational line of H_2 (adapted from Cabrit et al. 1998) with CO(2–1) contours superimposed (from Bachiller and Pérez Gutiérrez 1997).

In four out of the five outflows studied by Nisini et al. (1998), the FIR CO luminosity represents 10–30% of the flow kinetic luminosity, in good agreement with C-shock calculations in the inferred density and velocity range (Kaufman and Neufeld 1996). The only large discrepancy is observed in IC 1396N, an object contaminated by photodissociation region (PDR) emission (Molinari et al. 1998*a*). In L1157, the H_2 luminosity of warm gas is also around 10% of L_{CO} (Cabrit et al. 1998). Hence, these slow shocks seem sufficient to drive the whole outflows. Detailed comparisons between H_2 and FIR-CO lines in the same objects are now under way to narrow the range of possible shock models further and perhaps allow us to discriminate between wide-angle wind and jet scenarios for the entrainment of outflows.

V. CONCLUSIONS

We have shown that the current data on the structure and energetics of molecular outflows suggest broad similarities across the entire luminosity

range, from 1 to 10^5 $L_\odot$. If the flows are swept up by a stellar wind or jet, we find that $\dot{M}_w v_w / \dot{M}_a v_K$ has a value of about 0.3 for all flows, perhaps suggesting that flows have a common drive mechanism. However, it remains unclear whether the MHD disk and x-wind models that have been used to explain low-mass outflows are appropriate in the very different physical regime of high-mass YSOs. While observational data continue to improve these constraints, there remains an urgent need for a larger sample of molecular outflows, particularly from high-mass stars, to be fully mapped at high resolution; at the moment it is very possible that our estimates of the properties of high-mass systems are biased by strong selection effects. Single-dish data, especially from the new focal-plane arrays, plus interferometric images at millimeter wavelengths will continue to accumulate. However, only when the large millimeter interferometer (ALMA) is operational will it be possible to acquire high-resolution data quickly enough to study large samples of outflows in detail.

The nature of the shocks that drive outflows is slowly becoming clearer. We now have diagnostics of all the temperature components in the outflows, from the 2000-K gas seen in the 2-μm H_2 lines through the several-hundred-kelvin component recently detected by ISO, to the cool massive component seen in the millimeter waveband, where most of the momentum is eventually deposited. The relationship between these components is providing valuable tests of the outflow mechanism, although a fuller understanding will require observations at higher angular resolution than ISO provided. The SOFIA and especially the FIRST missions will provide valuable data in this area.

Acknowledgments D. S. S. would like to thank Andy Gibb and Chris Davis for providing unpublished outflow data for a number of sources and A. Gibb, A. Sargent, and L. Testi for useful discussions. J. S. R. acknowledges support from the Royal Society.

REFERENCES

Acord, J. M., Walmsley, C. M., and Churchwell, E. 1997. The extraordinary outflow toward G5.89 − 0.39. *Astrophys. J.* 475:693–704.

Bachiller, R. 1996. Bipolar molecular outflows from young stars and protostars. *Ann. Rev. Astron. Astrophys.* 34:111–154.

Bachiller, R., and Pérez Gutiérrez, M. 1997. Shock chemistry in the young bipolar outflow L1157. *Astrophys. J. Lett.* 487:93–97.

Bachiller, R., Cernicharo, J., Martín-Pintado, J., Tafalla, M., and Lazareff, B. 1990. High-velocity molecular bullets in a fast bipolar outflow near L1448/IRS3. *Astron. Astrophys.* 231:174–186.

Bachiller, R., Martín-Pintado, J., and Fuente, A. 1993. High-velocity hot ammonia in bipolar outflows. *Astrophys. J. Lett.* 417:45–48.

Bachiller, R., Tafalla, M., and Cernicharo, J. 1994. Successive ejection events in the L1551 molecular outflow. *Astrophys. J. Lett.* 425:93–96.

Bachiller, R., Guilloteau, S., Dutrey, A., Planesas, P., and Martín-Pintado, J. 1995. The jet-driven molecular outflow in L1448. CO and continuum synthesis images. *Astron. Astrophys.* 299:857–868.

Bachiller, R., Codella, C., Colomer, F., Liechti, S., and Walmsley, C. M. 1998. Methanol in protostellar outflows. Single-dish and interferometric maps of NGC 1333/IRAS 2. *Astrophys. J.* 335:266–276.

Bally, J., Devine, D., Hereld, M., and Rauscher, B. J. 1993. Molecular hydrogen in the IRAS 03282+3035 stellar jet. *Astrophys. J. Lett.* 418:75–78.

Bence, S. J., Richer, J. S., and Padman, R. 1996. RNO 43: A jet-driven super outflow. *Mon. Not. Roy. Astron. Soc.* 279: 866–883.

Bence, S. J., Padman, R., Isaak, K. G., Wiedner, M. C., and Wright, G. S. 1998. L43: The late stages of a molecular outflow. *Mon. Not. Roy. Astron. Soc.* 299:965–976.

Bergin, E. A., Neufeld, D. A., and Melnick, G. J. 1998. The postshock chemical lifetimes of outflow tracers and a possible new mechanism to produce water ice mantles. *Astrophys. J.* 499:777–792.

Blake, G.A. 1997. High angular resolution observations of the gas phase composition of young stellar objects. In *Molecules in Astrophysics: Probes and Processes*, IAU Symp. 178 (Dordrecht: Kluwer), ed. E. van Dishoeck, pp. 31–44.

Blake, G. A., van Dishoeck, E. F., Jansen, D. J., Groesbeck, T. D., and Mundy, L. G. 1994. Molecular abundances and low-mass star formation. 1: Si- and S-bearing species toward IRAS 16293−2422. *Astrophys. J.* 428:680–692.

Blake, G. A., Sandell, G., van Dishoeck, E. F., Groesbeck, T. D., Mundy, L. G., and Aspin, C. 1995. A molecular line study of NGC 1333/IRAS 4. *Astrophys. J.* 441:689–701.

Bontemps, S., André, P., Terebey, S., and Cabrit, S. 1996. Evolution of outflow activity around low-mass young stellar objects. *Astron. Astrophys.* 311:858–872.

Cabrit, S., and Bertout, C. 1992. CO line formation in bipolar flows. 3. The energetics of molecular flows and ionized winds. *Astron. Astrophys.* 261:274–284.

Cabrit, S., Goldsmith, P. F., and Snell, R. L. 1988. Identification of RNO 43 and B335 as two highly collimated bipolar flows oriented nearly in the plane of the sky. *Astrophys. J.* 334:196–208.

Cabrit, S., Raga, A., and Gueth, F. 1997. Models of bipolar molecular outflows. In *Herbig-Haro Flows and the Birth of Low Mass Stars*, IAU Symp. 182, ed. B. Reipurth and C. Bertout (Dordrecht: Kluwer), pp. 163–180.

Cabrit, S., Couturier, P., Andre, P., Boulade, O., Cesarsky, C. J., and Lagage, P. O., Sauvage, M., Bontemps, S., Nordh, L., Olofsson, G., Boulanger, F., Sibille, F., and Siebenmorgen, R. 1998. Mid-infrared emission maps of bipolar outflows with ISOCAM: An in-depth study of the L1157 outflow. In *Star Formation with the Infrared Space Observatory,* ASP Conf. Ser. 132, ed. J. Yun and R. Liseau (San Francisco Astronomical Society of the Pacific), pp. 326–329.

Ceccarelli, C., Haas, M. R., Hollenbach, D. J., and Rudolph, A. L. 1997. OI 63 micron-determined mass-loss rates in young stellar objects. *Astrophys. J.* 476:771–780.

Cernicharo, J., and Reipurth, B. 1996. Herbig-Haro jets, CO flows, and CO bullets: The case of HH 111. *Astrophys. J. Lett.* 460:57–61.

Cesaroni, R., Felli, M., Testi, L., Walmsley, C. M., and Olmi, L. 1997. The disk-outflow system around the high-mass (proto)star IRAS 20126+4104. *Astron. Astrophys.* 325:725–744.

Chandler, C. J., Terebey, S., Barsony, M., Moore, T. J. T., and Gautier, T. N. 1996. Compact outflows associated with TMC-1 and TMC-1A. *Astrophys. J.* 471:308–320.
Charnley, S. B. 1997. Sulfuretted molecules in hot cores. *Astrophys. J.* 481:396–405.
Chernin, L. M., and Masson, C. R. 1991. A nearly unipolar CO outflow from the HH 46-47 system. *Astrophys. J. Lett.* 382:93–96.
Chernin, L. M., and Wright, M. C. H. 1996. High-resolution CO observations of the molecular outflow in the Orion IRc2 region. *Astrophys. J.* 467:676–683.
Chernin, L., Masson, C., Gouveia Dal Pino, E. M., and Benz, W. 1994. Momentum transfer by astrophysical jets. *Astrophys. J.* 426:204–214.
Chièze, J.-P., Pineau des Forêts, G., and Flower, D. R. 1998. Temporal evolution of MHD shocks in the interstellar medium. *Mon. Not. Roy. Astron. Soc.* 295:672–682.
Churchwell, E. 1997*b*. Origin of the mass in massive star outflows. *Astrophys. J. Lett.* 479:59–61.
Cohen, M., Hollenbach, D. J., Haas, M. R., and Erickson, E. F. 1988. Observations of the 63 micron forbidden O I line in Herbig-Haro objects. *Astrophys. J.* 329:863–873.
Davis, C. J., and Eislöffel, J. 1995. Near-infrared imaging in H_2 of molecular (CO) outflows from young stars. *Astron. Astrophys.* 300:851–869.
Davis, C. J., Mundt, R., Ray, T. P., and Eislöffel, J. 1995. Near-infrared and optical imaging of the L1551-IRS5 region—The importance of poorly collimated outflows from young stars. *Astron. J.* 110:766–775.
Davis, C. J., Moriarty-Schieven, G., Eislöffel, J., Hoare, M. G., and Ray, T. P. 1998. Observations of shocked H_2 and entrained CO in outflows from luminous young stars. *Astron. J.* 115:1118–1134.
Devine, D., Bally, J., Reipurth, B., and Heathcote, S. 1997. Kinematics and evolution of the giant HH34 complex. *Astron. J.* 114:2095–2111.
Devine, D., Bally, J., Reipurth, B., Shepherd, D. S., and Watson, A. M. 1999. A giant Herbig-Haro flow from a massive young star in G192.16−3.82. *Astron. J.*, in press.
Doyon, R., and Nadeau, D. 1988. The molecular hydrogen emission from the Cepheus A star-formation region. *Astrophys. J.* 334:883–890.
Draine, B. T., and McKee, C. F. 1993. Theory of interstellar shocks. *Ann. Rev. Astron. Astrophys.* 31:373–432.
Dutrey, A., Guilloteau, S., and Bachiller, R. 1997. Successive SiO shocks along the L1448 jet axis. *Astron. Astrophys.* 325:758–768.
Dyson, J. E. 1984. The interpretation of flows in molecular clouds. *Astrophys. Space Sci.* 106:181–197.
Eislöffel, J., and Davis, C. J., 1995. Near-infrared imaging in H_2 of molecular (CO) outflows from young stars. *Astrophys. Space Sci.* 233:59–62.
Eislöffel, J., Davis, C. J., Ray, T. P., and Mundt, R. 1994. Near-infrared observations of the HH 46/47 system. *Astrophys. J. Lett.* 422:91–93.
Ferreira, J. 1997. Magnetically-driven jets from Keplerian accretion discs. *Astron. Astrophys.* 319:340–359.
Fiege, J. D., and Henriksen, R. N. 1996*a*. A global model of protostellar bipolar outflow—I. *Mon. Not. Roy. Astron. Soc.* 281:1038.
Fiege, J. D., and Henriksen, R. N. 1996*b*. A global model of protostellar bipolar outflow—II. *Mon. Not. Roy. Astron. Soc.* 281:1055.
Flower, D. R., and Pineau des Forêts, G. 1994. Grain-mantle erosion in magneto-hydrodynamic shocks. *Mon. Not. Roy. Astron. Soc.* 268:724.
Flower, D. R., Pineau des Forêts, G., Field, D., and May, P. W. 1996. The structure of MHD shocks in molecular outflows: Grain sputtering and SiO formation. *Mon. Not. Roy. Astron. Soc.* 280:447.

Fridlund, C. V. M., and Liseau, R. 1998. Two jets from the protostellar system L1551 IRS5. *Astrophys. J. Lett.* 599:75–77.

Fukui, Y., Iwata, T., Mizuno, A., Bally, J., and Lane, A. P. 1993. Molecular outflows. In *Protostars and Planets III*, ed. E. H. Levy and J. I. Lunine (Tucson: University of Arizona Press), pp. 603–639.

Garay, G., Ramirez, S., Rodríguez, L. F., Curiel, S., and Torrelles, J. M. 1996. The nature of the radio sources within the Cepheus A star-forming region. *Astrophys. J.* 459:193–208.

Gayley, K. G., Owocki, S. P., and Cranmer, S. R. 1995. Momentum deposition in Wolf-Rayet winds: Nonisotropic diffusion with effective gray opacity. *Astrophys. J.* 442:296–310.

Glassgold, A. E., Mamon, G. A., and Huggins, P. J. 1989. Molecule formation in fast neutral winds from protostars. *Astrophys. J. Lett.* 336:29–31.

Gredel, R. 1994. Near-infrared spectroscopy and imaging of Herbig-Haro objects. *Astron. Astrophys.* 292:580–592.

Gueth, F., and Guilloteau, S. 1999. The jet-driven molecular outflow of HH211. *Astron. Astrophys.* 343:571–584.

Gueth, F., Guilloteau, S., and Bachiller, R. 1996. A precessing jet in the L1157 molecular outflow. *Astron. Astrophys.* 307:891–897.

Guilloteau, S., Bachiller, R., Fuente, A., and Lucas, R. 1992. First observations of young bipolar outflows with the IRAM interferometer—2 arcsec resolution SiO images of the molecular jet in L1448. *Astron. Astrophys. Lett.* 265:49–52.

Hartigan, P., Morse, J., and Raymond, J. 1994. Mass loss rates, ionization fractions, shock velocities and magnetic fields of stellar jets. *Astrophys. J.* 436:125–143.

Hartigan, P., Carpenter, J. M., Dougados, C., and Skrutskie, M. F. 1996. Jet bow shocks and clumpy shells of H_2 emission in the young stellar outflow Cepheus A. *Astron. J.* 111:1278–1285.

Henriksen, R.N. 1994. Theory of bipolar outflows. In *The Cold Universe*, ed. T. Montmerle, C. J. Lada, I. F. Mirabel, and J. Tran Thanh Van (Gif-sur-Yvette: Editions Frontières), pp. 241–253.

Hollenbach, D. 1985. Mass loss rates from protostars and OI (63 micron) shock luminosities. *Icarus* 61:36–39.

Hollenbach, D. 1997. The physics of molecular shocks in YSO outflows. In *Herbig-Haro Flows and the Birth of Low-Mass Stars*, IAU Symp. 182, ed. B. Reipurth and C. Bertout (Dordrecht: Kluwer), pp. 181–198.

Hughes, S.M.G. 1993. Is Cepheus A East a Herbig-Haro object? *Astron. J.* 105:331–338.

Kameya, O., Hasegawa, T. I., Hirano, N., and Takakubo, K. 1989. High velocity flows in the NAC7538 molecular cloud. *Astrophys. J.* 339:222–230.

Kaufman, M. J., and Neufeld, D. A. 1996. Far-infrared water emission from magnetohydrodynamic shock waves. *Astrophys. J.* 456:611–630.

Kelly, M. L., and Macdonald, G. H. 1996. Two new young stellar objects with bipolar outflows in L379. *Mon. Not. Roy. Astron. Soc.* 282:401–412.

Lada, C. J., and Fich, M. 1996. The structure and energetics of a highly collimated bipolar outflow: NGC 2264G. *Astrophys. J.* 459:638–652.

Langer, W. D., Castets, A., and Lefloch, B. 1996. The IRAS 2 and IRAS 4 outflows and star formation in NGC 1333. *Astrophys. J. Lett.* 471:L111—L115.

Liseau, R., Giannini, T., Nisini, B., Saraceno, P., Spinoglio, L., Larsson, B., Lorenzetti, D., and Tommasi, E. 1997. Far-IR spectrophotometry of HH flows with the ISO long-wavelength spectrometer. In *Herbig-Haro Flows and the Birth of Low Mass Stars*, IAU Symp. 182, ed. B. Reipurth and C. Bertout (Dordrecht: Kluwer), pp. 111–120.

Martí, J., Rodríguez, L. F., and Reipurth, B. 1993. HH 80-81: A highly collimated Herbig-Haro complex powered by a massive young star. *Astrophys. J.* 416:208–217.
Martí, J., Rodríguez, L. F., and Reipurth, B. 1995. Large proper motions and ejection of new condensations in the HH 80-81 thermal radio jet. *Astrophys. J.* 449:184-187.
Martín-Pintado, J., Bachiller, R., and Fuente, A. 1992. SiO emission as a tracer of shocked gas in molecular outflows. *Astron. Astrophys.* 254:315–326.
Masson, C. R., and Chernin, L. M. 1992. Properties of swept-up molecular outflows. *Astrophys. J. Lett.* 387:L47–L50.
Masson, C. R., and Chernin, L. M. 1993. Properties of jet-driven molecular outflows. *Astrophys. J.* 414:230–241.
Masson, C. R., and Chernin, L. M. 1994. Observational constraints on outflow models. In *Clouds, Cores, and Low-Mass Stars*, ASP Conf. Ser. 65, ed. D. Clemens and R. Barvainis (San Francisco: Astronomical Society of the Pacific), pp. 350–359.
McCaughrean, M., and Mac Low, M.-M. 1997. The OMC-1 molecular hydrogen outflow as a fragmented stellar wind bubble. *Astron. J.* 113:391–400.
McCaughrean, M. J., Rayner, J. T., and Zinnecker, H. 1994. Discovery of a molecular hydrogen jet near IC 348. *Astrophys. J. Lett.* 436:L189–L192.
Mellema, G., and Frank, A. 1997. Outflow collimation in young stellar objects. *Mon. Not. Roy. Astron. Soc.* 292:795–807.
Micono, M., Davis, C. J., Ray, T. P., Eislöffel, J., Shetrone, M. D. 1998. Proper motions and variability of the H_2 emission in the HH 46/47 system. *Astrophys. J. Lett.* 494:L227–L230.
Mitchell, G. F., Maillard, J. P., and Hasegawa, T. I. 1991. Episodic outflows from high-mass protostars. *Astrophys. J.* 371:342–356.
Mitchell, G. F., Hasegawa, T. I., Dent, W.R.F., and Matthews, H. E. 1994. A molecular outflow driven by an optical jet. *Astrophys. J. Lett.* 436:177–180.
Mitchell, G. F., Lee, S. W., Maillard, J. P., Matthews, H. E., Hasegawa, T. I., and Harris, A. I. 1995. A multitransitional CO study of GL 490. *Astrophys. J.* 438:794–812.
Molinari, S., Saraceno, P., Nisini, B., Giannini, T., Ceccarelli, C., White, G. J., Caux, E., and Palla, F. 1998*a*. Shocks and PDRs in an intermediate mass star forming globule: The case of IC1396N. *Star Formation with the Infrared Space Observatory,* in ASP Conf. Ser. 132, ed. J. Yun and R. Liseau (San Francisco: Astronomical Society of the Pacific), pp. 390–394.
Molinari, S., Testi, L., Brand, J., Cesaroni, R., and Palla, F. 1998*b*. IRAS 23385 +6053: A prototype massive Class 0 object. *Astrophys. J. Lett.* 505:39–42.
Moriarty-Schieven, G. H., and Snell, R. L. 1988. High-resolution images of the L1551 molecular outflows. II. Structure and kinematics. *Astrophys. J.* 332:364–378.
Mundt, R., Brugel, E. W., and Bührke, T. 1987. Jets from young stars: CCD imaging, long-slit spectroscopy and interpretation of existing data. *Astrophys. J.* 319:275–303.
Nagar, N. M., Vogel, S. N., Stone, J. M., and Ostriker, E. C. 1997. Kinematics of the molecular sheath of the HH 111 optical jet. *Astrophys. J. Lett.* 482:195–198.
Narayanan, G., and Walker, C. K. 1996. Evidence for multiple outbursts from the Cepheus A molecular outflow. *Astrophys. J.* 466:844–865.
Netzer, N., and Elitzur, M. 1993. The dynamics of stellar outflows dominated by interaction of dust and radiation. *Astrophys. J.* 410:701–713.
Nisini, B., Lorenzetti, D., Cohen, M., Ceccarelli, C., Giannini, T., Liseau, R., Molinari, S., Radicchi, A., Saraceno, P., Spinoglio, L., Tommasi, E., Clegg, P. E., Ade, P.A.R., Armand, C., Barlow, M. J., Burgdorf, M., Caux, E., Cerulli,

P., Church, S. E., di Giorgio, A., Fischer, J., Furniss, I., Glencross, W. M., Griffin, M. J., Gry, C., King, K. J., Lim, T., Naylor, D. A., Texier, D., Orfei, R., Nguyen-Q-Rieu, Sidher, S., Smith, H. A., Swinyard, B. M., Trams, N., Unger, S. J., and White, G. J. 1996. LWS-spectroscopy of Herbig Haro objects and molecular outflows in the Cha II dark cloud. *Astron. Astrophys.* 315:L321–L324.

Nisini, B., Giannini, T., Molinari, S., Saraceno, P., Caux, E., Ceccarelli, C., Liseau, R., Lorenzetti, D., Tommasi, E. and White, G. J. 1998. High-J CO lines from YSOs driving molecular outflows. In *Star Formation with the Infrared Space Observatory*, ASP Conf. Ser. 132, ed. J. Yun and R. Liseau (San Francisco: Astronomical Society of the Pacific), pp. 256–264.

Padman, R., and Richer, J. S. 1994. Interactions between molecular outflows and optical jets. *Astrophys. Space Sci.* 216:129–134.

Padman, R., Bence, S., and Richer, J. 1997. Observational properties of molecular outflows. In *Herbig-Haro Flows and the Birth of Low Mass Stars,* IAU Symp. 182, ed. B. Reipurth and C. Bertout (Dordrecht: Kluwer), pp. 123–140.

Panagia, N. 1991. Ionized winds from young stellar objects. In *The Physics of Star Formation and Early Stellar Evolution*, ed. C. J. Lada and N. Kylafis (Dordrecht: Kluwer), pp. 565–593.

Pismis, P., and Torres-Peimbert, S. 1995. *Revista Mexicana de Astronomía y Astrofísica Serie de Conferencías* vol. 1.

Poetzel, R., Mundt, R., and Ray, T. P. 1989. Z CMa—a large-scale high velocity bipolar outflow traced by Herbig-Haro objects and a jet. *Astron. Astrophys. Lett.* 224:13–16.

Raga, A. 1991. A new analysis of the momentum and mass-loss rates of stellar jets. *Astron. J.* 101:1472–1475.

Raga, A. C., Cantó, J., Calvet, N., Rodríguez, L. F., and Torrelles, J. M. 1993. A unified stellar jet/molecular outflow model. *Astron. Astrophys.* 276:539–548.

Raga, A. C., Taylor, S. D., Cabrit, S., and Biro, S. 1995. A simulation of an HH jet in a molecular environment. *Astron. Astrophys.* 296:833–843.

Reipurth, B., and Bertout, C. 1997. *Herbig-Haro Flows and the Birth of Low-Mass Stars,* IAU Symp. 182 (Dordrecht: Kluwer).

Reipurth, B., Bally, J., and Devine, D. 1997. Giant Herbig-Haro flows. *Astron. J.* 114:2708–2735.

Richer, J. S., Hills, R. E., Padman, R., and Russell, A.P.G. 1989. High-resolution molecular line observations of the core and outflow in Orion B. *Mon. Not. Roy. Astron. Soc.* 241:231–246.

Richer, J. S., Hills, R. E., and Padman, R. 1992. A fast CO jet in Orion B. *Mon. Not. Roy. Astron. Soc.* 254:525–538.

Rodríguez, L. F. 1995. Subarcsecond observations of radio continuum from jets and disks. *Rev. Mex. Astron. Astrofís. Ser. Conf.* 1:1–10.

Rodríguez, L. F., Carral, P., Moran, J. M., and Ho, P. T. P. 1982. Anisotropic mass outflow in regions of star formation. *Astrophys. J.* 260:635–646.

Rodríguez, L. F., Garay, G., Curiel, S., Ramírez, S., Torrelles, J. M., Gómez, Y., and Velázquez, A. 1994. Cepheus A HW2: A powerful thermal radio jet. *Astrophys. J. Lett.* 430:L65–L68.

Russell, A. P. G., Bally, J., Padman, R., and Hills, R. E. 1992. Atomic and molecular outflow in DR 21. *Astrophys. J.* 387:219–228.

Saraceno, P., André, P., Ceccarelli, C., Griffin, M., and Molinari, S. 1996. An evolutionary diagram for young stellar objects. *Astron. Astrophys.* 309:827–839.

Saraceno, P., Nisini, B., Benedettini, M., Ceccarelli, C., di Giorgio, A. M., Giannini, T., Molinari, S., Spinogl, L., Clegg, P. E., Correia, J. C., Griffin, M. J., Leeks, S. J., White, G. J., Caux, E., Lorenzetti, D., Tommasi, E., Liseau, R., and Smith, H. A. 1998. LWS observations of pre–main sequence objects.

In *Star Formation with the Infrared Space Observatory*, ASP Conf. Ser. 132, ed. J. Yun and R. Liseau (San Francisco Astronomical Society of the Pacific), pp. 233–237.
Shepherd, D. S., and Churchwell, E. 1996. Bipolar molecular outflows in massive star-formation regions. *Astrophys. J.* 472:225–239.
Shepherd, D. S., and Kurtz, S. E. 1999. A 1000-AU rotating disk around the massive young stellar object a192.16. *Astrophys. J.* in press
Shepherd, D. S., Watson, A. M., Sargent, A. I., and Churchwell, E. 1998. Outflows and luminous YSOs: A new perspective on the G192.16 massive bipolar outflow. *Astrophys. J.* 507:861–873.
Shu, F. H., and Shang, H. 1997. Protostellar X-rays, jets, and bipolar outflows. In *Herbig-Haro Flows and the Birth of Low-Mass Stars,* IAU Symp. 182, ed. B. Reipurth and C. Bertout (Dordrecht: Kluwer), pp. 225–239.
Shu, F. H., Ruden, S. P., Lada, C. J., and Lizano, A. 1991. Star formation and the nature of bipolar outflows. *Astrophys. J. Lett.* 370:L31–L34.
Shu, F., Najita, J., Ostriker, E., Wilkin, F., Ruden, S., and Lizano, S. 1994. Magnetocentrifugally driven flows from young stars and disks. 1: A generalized model. *Astrophys. J. Lett.* 429:781–796.
Smith, M. D. 1994. Jump shocks in molecular clouds—speed limits and excitation levels. *Mon. Not. Roy. Astron. Soc.* 266:238–246.
Smith, M. D., Suttner, G., and Yorke, H. W. 1997. Numerical hydrodynamic simulation of jet-driven bipolar outflows. *Astron. Astrophys.* 323:223–230.
Smith, M. D., Eislöffel, J., and Davis, C. J. 1998. ISO observations of molecular hydrogen in the DR21 bipolar outflow. *Mon. Not. Roy. Astron. Soc.* 297:687–691.
Stahler, S. W. 1994. The kinematics of molecular outflows. *Astrophys. J.* 422:616–620.
Stone, J. M., Xu, J., and Mundy, L. G. 1995. Formation of bullets by hydrodynamical instabilities in stellar outflow. *Nature* 377:315–317.
Suttner, G., Smith, M. D., Yorke, H. W., and Zinnecker, H. 1997. Multi-dimensional numerical simulations of molecular jets. *Astron. Astrophys.* 318:595–607.
Tafalla, M., and Bachiller, R. 1995. Ammonia emission from bow shocks in the L1157 outflow. *Astrophys. J. Lett.* 443:37–40.
Taylor, S. D., and Raga, A. C. 1995. Molecular mixing layers in stellar outflows. *Astron. Astrophys.* 296:823–832.
Torrelles, J. M., Verdes-Montenegro, L., Ho, P. T. P., Rodríguez, L. F., and Jorge, C. 1993. From bipolar to quadrupolar—the collimation processes of the Cepheus A outflow. *Astrophys. J.* 410:202–217.
van Dishoeck, E. F., and Blake, G. A. 1998. Chemical evolution of star-forming regions. *Ann. Rev. Astron. Astrophys.,* 36:317–368.
van Dishoeck, E. F., Blake, G. A., Jansen, D. J., and Groesbeck, T. D. 1995. Molecular abundances and low-mass star formation. II. Organic and deuterated species toward IRAS 16293-2422. *Astrophys. J.* 447:760–787.
Velusamy, T., and Langer, W. D. 1998. Outflow-infall interactions as a mechanism for terminating accretion in protostars. *Nature* 392:685–687.
Wright, C. M., Drapatz, S., Timmermann, R., Van Der Werf, P. P., Katterloher, R., and De Graauw, T. 1996. Molecular hydrogen observations of Cepheus A West. *Astron. Astrophys. Lett.* 315:L301–L304.
Wu, Y., Huang, M., and He, J. 1996. A catalogue of high velocity molecular outflows. *Astron. Astrophys. Suppl.* 115:283–284.
Yamashita, T., Suzuki, H., Kaifu, N., Tamura, M., Mountain, C. M., and Moore, T. J. T. 1989. A new CO bipolar flow and dense disk system associated with the infrared reflection nebula GGD 27 IRS. *Astrophys. J.* 347:894–900.
Zhang, Q., Hunter, T. R., and Sridharan, T. K. 1998. A rotating disk around a high-mass young star. *Astrophys. J. Lett.* 505:L151–L154.